CentroidKV: Efficient Long-Context LLM Inference via KV Cache Clustering

Anonymous authors
Paper under double-blind review

Abstract

Large language models (LLMs) with extended context windows have become increasingly prevalent for tackling complex tasks. However, the substantial Key-Value (KV) cache required for long-context LLMs poses significant deployment challenges. Existing approaches either discard potentially critical information needed for future generations or offer limited efficiency gains due to high computational overhead. In this paper, we introduce *CentroidKV*, a simple yet effective framework for online KV cache clustering. Our approach is based on the observation that key states exhibit high similarity along the sequence dimension. To enable efficient clustering, we divide the sequence into chunks and propose *Chunked Soft Matching*, which employs an alternating partition strategy within each chunk and identifies clusters based on similarity. CentroidKV then merges the KV cache within each cluster into a single centroid. Additionally, we provide a theoretical analysis of the computational complexity and the optimality of the intra-chunk partitioning strategy. Extensive experiments across various models and long-context benchmarks demonstrate that CentroidKV achieves up to 75% reduction in KV cache memory usage while maintaining comparable model performance. Moreover, with minimal computational overhead, CentroidKV accelerates the decoding stage of inference by up to 3.19× and reduces end-to-end latency by up to 2.72×.

1 Introduction

With the increasing demand to tackle a diverse range of complex real-world applications, such as multi-round dialogues (Thoppilan et al., 2022), Large Language Models (LLMs) have been capable of supporting context windows of up to 1M tokens (Achiam et al., 2023; Touvron et al., 2023; Team et al., 2024). However, deploying LLMs in long-context scenarios introduces substantial challenges, particularly related to the Key-Value (KV) cache. The KV cache stores the keys and values of all preceding tokens to avoid re-computation, and its memory requirements scale linearly with the context length. Due to the auto-regressive nature of LLMs, generating each token necessitates accessing the entire KV cache, making it a significant bottleneck for both inference latency and throughput. Moreover, the large size of KV cache imposes considerable demands on memory capacity, further complicating deployment.

To address these challenges, there is a pressing need for effective methods to reduce the KV cache size. Existing studies have explored this problem from multiple perspectives, including KV cache eviction (Zhang et al., 2023; Xiao et al., 2023; Ge et al., 2023; Li et al., 2024; Liu et al., 2024b; Yang et al., 2024; Cai et al., 2024), KV cache merging (Zhang et al.; Wang et al., 2024; Wan et al., 2024), quantization (Hooper et al., 2024; Liu et al., 2024c), and channel pruning (Xu et al., 2024), among others. By leveraging the inherent sparsity of the attention score matrix (Zhang et al., 2023), various methods have been proposed to reduce redundancy along the sequence length dimension. However, these approaches exhibit notable limitations. KV cache eviction, which discards less critical tokens based on historical attention scores, often leads to significant performance degradation. This occurs because tokens deemed unimportant in the current context may become crucial for future generations, especially in long-context scenarios. To improve the model performance after eviction, recent works (Yang et al., 2024; Cai et al., 2024; Tang et al., 2024; Feng et al., 2024; Xiao et al., 2024; Shi et al., 2024) allocate different KV cache budget across layers and attention heads. Additionally, subsequent methods such as (Zhang et al.) merge the tokens to be evicted with the tokens to be retained.

However, existing methods typically rely on preliminary token eviction to define merging sets, which often forces semantically distant tokens to be grouped together, resulting in centroid bias and information loss, ultimately degrading model performance. In contrast, our approach aims to compress the KV cache by clustering them into centroids based on the intrinsic similarity.

Our approach is inspired by a key observation: key states exhibit high similarity along the sequence dimension, as illustrated in Figure 2. This insight motivates us to cluster the KV cache by identifying merging sets solely based on token similarity. However, efficiently and accurately performing KV cache clustering online remains challenging, particularly given the long sequence lengths involved.

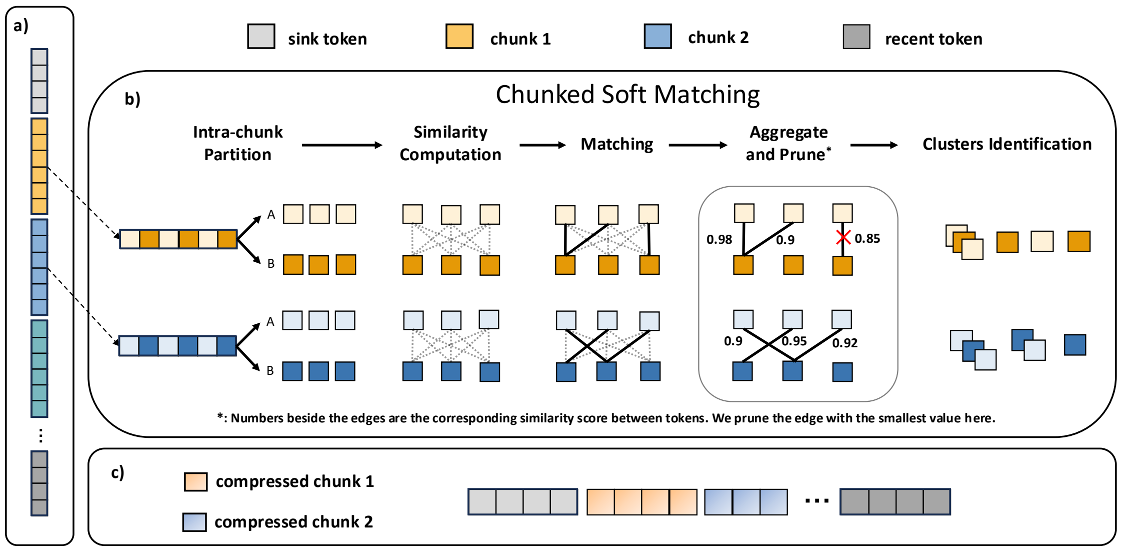

Figure 1: An overview of CentroidKV: a) Divide sequences into chunks; b) Chunked Soft Matching to identify clusters; c) KV cache compression after clustering.

In this paper, we introduce *CentroidKV*, a simple yet effective online KV cache clustering framework that improves the inference efficiency of LLMs in long-context scenarios. The core innovation of CentroidKV is the *Chunked Soft Matching* algorithm, which enables efficient KV cache clustering without compromising model performance. Inspired by the Bipartite Soft Matching algorithm (Bolya et al., 2022) for Vision Transformers (Dosovitskiy, 2020), we are the first to extend this idea to the context of KV cache compression. Given the cache budget, one clustering round is executed as follows. The framework begins by dividing the sequence into chunks. Based on the observed correlation between token similarity and positional distance, we further partition each chunk in an alternating manner and theoretically prove the optimality of this intra-chunk partitioning strategy. Subsequently, *Chunked Soft Matching* identifies clusters by locating highly similar token pairs across all chunks. Finally, the corresponding keys and values within each cluster are merged into a single centroid. As the decoding process advances, CentroidKV calls the clustering process if the cache size exceeds the budget.

We conduct extensive experiments on popular models to evaluate both the effectiveness and efficiency of CentroidKV. The results demonstrate that CentroidKV can reduce the KV cache memory usage by up to 75% while maintaining comparable model performance. Furthermore, by dynamically clustering to preserve contextual information, CentroidKV outperforms baselines under a limited cache budget. Additionally, due to its simplicity and efficiency, CentroidKV accelerates the decoding stage of LLM inference by up to 3.19× and reduces end-to-end latency by up to 2.72×.

Our contributions are summarized as follows.

- We introduce *CentroidKV*, a simple yet effective framework for online KV cache clustering. The core innovation is a novel clustering algorithm, termed *Chunked Soft Matching*.

- CentroidKV is a lightweight, plug-and-play solution to improve LLM inference efficiency. We theoretically analyze its computational complexity and formally prove the optimality of the intra-chunk partitioning strategy based on the observed similarity patterns.
- CentroidKV achieves up to an 75% reduction in KV cache memory usage with minimal impact on model performance. Additionally, it accelerates the decoding stage by up to 3.19× and reduces end-to-end latency by up to 2.72×.

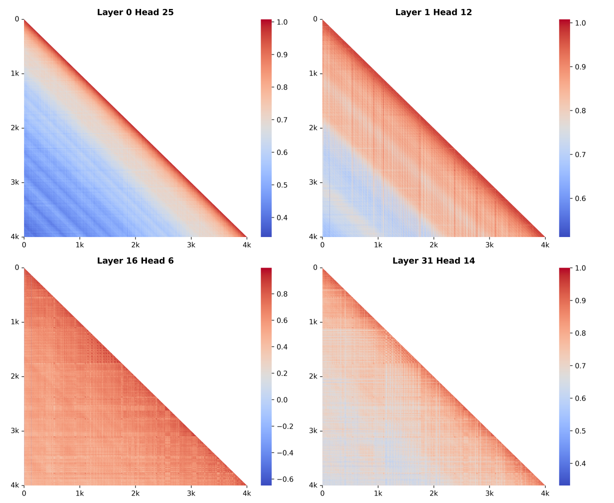

Figure 2: The cosine similarity maps of key states across various layers and heads.

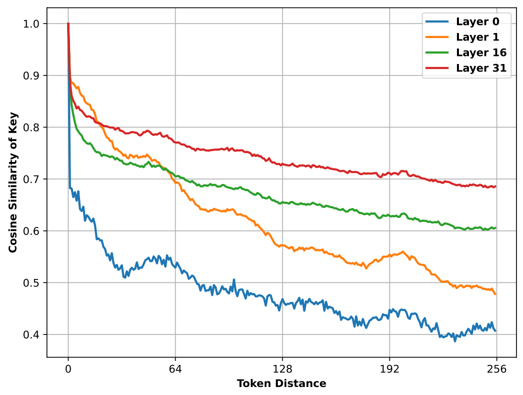

Figure 3: The correlation between token distance and the cosine similarity of key states.

2 Related Work

KV Cache Compression. Eviction-based approaches aim to maintain a fixed-size KV cache during decoding by selectively retaining informative tokens. H2O (Zhang et al., 2023) retains a limited budget of KV cache by greedily discarding unimportant tokens based on the accumulated attention score. StreamingLLM (Xiao et al., 2023) preserves the initial few tokens along with the recent tokens, based on the identification of attention sinks. SnapKV (Li et al., 2024) selects important tokens for each attention head based on the observation window of prompts. FastGen (Ge et al., 2023) conducts profiling for attention heads and dynamically evicts tokens based on different attention patterns. Despite their efficiency, these methods suffer from performance degradation in the long context scenario, since the information of the discarded token will be lost permanently. To mitigate this limitation, subsequent approaches (Zhang et al.; Wan et al., 2024) introduce compensation mechanisms that merge evicted tokens into the remaining cache. However, their reliance on preliminary eviction still constrains their ability to preserve full contextual information. ClusterKV (Liu et al., 2024a) employs K-means clustering to enhance the retrieval of salient tokens; however, the high computational overhead of iterative clustering procedures limits its practicality for latency-sensitive online inference scenarios. Another line of work, such as PyramidKV (Cai et al., 2024) and PyramidInfer (Yang et al., 2024), focuses on optimizing cache budget allocation across layers to improve overall model accuracy.

Bipartite Soft Matching. Introduced by ToMe (Bolya et al., 2022), Bipartite Soft Matching (BSM) is an algorithm designed to merge tokens in Vision Transformers (ViT) (Dosovitskiy, 2020), which is as fast as token pruning. Recent studies (Bolya & Hoffman, 2023; Kim et al., 2024; Tran et al., 2024) have extended BSM to enhance the efficiency of ViTs and Stable Diffusion (Rombach et al., 2022) without compromising model performance.

3 Preliminary

In this section, we first give a basic preliminary about the KV cache clustering in LLM inference. For simplicity, we focus on a single attention head within a specific layer. LLM inference consists of two stages: pre-filling and decoding. During the pre-filling stage, the model generates the first token and initializes the KV cache, which stores the key and value states of the prompt as $K \in \mathbb{R}^{n\times d}$ and $V \in \mathbb{R}^{n\times d}$, respectively. In the decoding stage, for the given states of the current input $q, k, v \in \mathbb{R}^{1\times d}$, KV cache is updated as $K = [K, k]$, $V = [V, v]$. The vanilla attention output is then computed as follows:

$$\mathrm{Attn}(q, K, V) = \mathrm{softmax}\left(\frac{qK^T}{\sqrt{d_k}}\right) V = \frac{\sum_{i=1}^{n} \exp\left(\frac{q^T k_i}{\sqrt{d_k}}\right) v_i}{\sum_{i=1}^{n} \exp\left(\frac{q^T k_i}{\sqrt{d_k}}\right)}. \tag{1}$$

For clearer derivation, we decompose KV cache into individual tokens, represented as $K = [k_1, \dots, k_n]$ and $V = [v_1, \dots, v_n]$, where each $k_i \in \mathbb{R}^d$ and $v_i \in \mathbb{R}^d$. In our approach, we utilize the cosine similarity as the distance metric between key states:

$$\cos(k_i, k_j) = \frac{k_i \cdot k_j}{\|k_i\|\|k_j\|} \tag{2}$$

Assume that tokens are grouped into clusters based on the similarity of their key states. The cluster centers are denoted as $\hat{K} = [\hat{k}_1, \dots, \hat{k}_C]$, where C represents the number of clusters. The number of tokens in each cluster is denoted by $N = [n_1, \dots, n_C]$, with each cluster center $\hat{k}_t$ associated with a set of tokens $[\hat{k}_{1,t}, \dots, \hat{k}_{n_t,t}]$, corresponding to the tokens in the t-th cluster. Here, n_t is referred to as the cluster degree.

By approximating the attention output using the cluster centers in place of the original key states, the resulting attention output is as follows:

$$\begin{aligned}
\mathrm{Attn}(q, K, V) &= \frac{\sum_{t=1}^{C}\sum_{i=1}^{n_t} \exp\left(\frac{q^T k_{i,t}}{\sqrt{d_k}}\right) v_{i,t}}{\sum_{t=1}^{C}\sum_{i=1}^{n_t} \exp\left(\frac{q^T k_{i,t}}{\sqrt{d_k}}\right)} \\
&\approx \frac{\sum_{t=1}^{C}\sum_{i=1}^{n_t} \exp\left(\frac{q^T \hat{k}_t}{\sqrt{d_k}}\right) v_{i,t}}{\sum_{t=1}^{C}\sum_{i=1}^{n_t} \exp\left(\frac{q^T \hat{k}_t}{\sqrt{d_k}}\right)} \\
&= \frac{\sum_{t=1}^{C}\left[\exp\left(\frac{q^T \hat{k}_t}{\sqrt{d_k}}\right)\sum_{i=1}^{n_t} v_{i,t}\right]}{\sum_{t=1}^{C} n_t \exp\left(\frac{q^T \hat{k}_t}{\sqrt{d_k}}\right)}.
\end{aligned}$$

By merging the value states corresponding to the same indices as the key states, namely $\hat{v}_t = \frac{\sum_{i=1}^{n_t} v_{i,t}}{n_t}$, we formulate the approximate attention output, denoted as AppAttn, as follows:

$$\begin{aligned}
\mathrm{Attn}(q, K, V) &\approx \frac{\sum_{t=1}^{C} n_t \exp\left(\frac{q^T \hat{k}_t}{\sqrt{d_k}}\right) \hat{v}_t}{\sum_{t=1}^{C} n_t \exp\left(\frac{q^T \hat{k}_t}{\sqrt{d_k}}\right)} \\
&= \frac{\sum_{t=1}^{C} \exp\left(\frac{q^T \hat{k}_t}{\sqrt{d_k}} + \log n_t\right) \hat{v}_t}{\sum_{t=1}^{C} \exp\left(\frac{q^T \hat{k}_t}{\sqrt{d_k}} + \log n_t\right)} \\
&\triangleq \mathrm{AppAttn}(q, \hat{K}, \hat{V}, N),
\end{aligned} \tag{3}$$

where $\hat{V} = [\hat{v}_1, \dots, \hat{v}_C]$. Equation (3) demonstrates that the approximate attention after clustering aligns with the vanilla attention in Equation (1) when each token is treated as a separate cluster. To minimize output error, it is essential that the key states within each cluster exhibit high similarity. Fortunately, the following observations further support the viability of this approach.

4 Observations

In this section, we present several empirical observations that motivate our approach.

Observation 1. Key states exhibit high, localized similarity along the sequence dimension.

Using the Llama-2-7B-32K model (Together, 2023), we randomly sample sequences of length 4K from the WikiText-2 (Merity et al., 2016) dataset and perform zero-shot inference. The cosine similarity maps of the key states are visualized in Figure 2. We observe that key states exhibit high cosine similarity between tokens across different layers and heads. Notably, tokens with high similarity tend to cluster within localized regions. These findings align with previous work (Wang et al., 2024).

This observation suggests that KV cache clustering can be leveraged for efficient inference without compromising accuracy. Furthermore, the observed localized similarity motivates us to subsequently enhance clustering efficiency by identifying similar tokens within local regions, rather than considering the entire sequence.

Observation 2. As token distance increases, the cosine similarity of key states generally decreases monotonically and follows a convex trend.

Building on the observed localized similarity, we further investigate the correlation between token distance and the cosine similarity of key states. We randomly sample multiple tokens within the sequence, define the local region as 256 tokens, and compute the average similarity across samples and attention heads. As illustrated in Figure 3, we find that as token distance increases, the cosine similarity between key states generally follows a monotonically decreasing trend. Furthermore, this correlation appears to be convex with respect to the distance.

This observation motivates our framework design of a highly efficient clustering algorithm that minimizes the computational complexity of identifying similar token sets. Additionally, it provides empirical support for the theoretical analysis in Section 6 which proves the optimality of the partitioning strategy in our framework.

5 Method

In this section, we introduce *CentroidKV*, a simple yet effective framework for KV cache clustering designed to enhance the efficiency of long-context LLM inference. The framework comprises three key steps. First, the sequence is divided into chunks while preserving the attention sinks and recent tokens. Second, we propose a novel KV cache clustering algorithm, termed *Chunked Soft Matching*, which employs an alternating partition strategy within each chunk and identifies clustering sets by finding highly similar token pairs across all chunks. Finally, the key and value states are merged based on the identified clusters, yielding a compressed KV cache for subsequent generations. An overview of CentroidKV is depicted in Figure 1.

5.1 Overall Inference Pipeline

The overall pipeline of LLM inference integrated with CentroidKV is illustrated in Algorithm 1. The cache budget B is determined by the prompt length n and the cache ratio R. In the pre-filling stage, after computing the attention output by Flash Attention (Dao et al., 2022), CentroidKV is invoked to conduct the first clustering if the KV cache size exceeds the budget, which compresses the KV cache to centroids and records the cluster degree. In the decoding stage, the KV cache grows by one token at each step, causing the memory budget to be exceeded continuously. To amortize the compression overhead and maintain inference efficiency, CentroidKV is invoked periodically every g decoding steps.

As illustrated in Figure 1, CentroidKV primarily employs the Chunked Soft Matching algorithm to compress the KV cache. The compression ratio r in Algorithm 1 governs the proportion of pruned edges in Figure 1. Since Bipartite Soft Matching can reduce the cache size by at most half in a single pass, multiple rounds of clustering are performed to progressively compress the KV cache until it meets the predefined budget.

Algorithm 1 Inference Pipeline with CentroidKV

```
**Require:** cache ratio $R$, compression ratio $r$, maximum decoding length $\Gamma$, attention sink $n_1$, recent budget $n_2$, interval step $g$, chunk size $c$.
**Pre-filling:** $Q, K, V \in \mathbb{R}^{n \times d}$.
Cache length $s = n$, Cluster degree $N = [1] \cdot n$, Cache budget $B = R \cdot n$.    ▷ Initialization
$O = \text{FlashAttn}(Q, K, V)$
**if** $s \geq B$ **then**
    $K, V, N, s = \text{CentroidKV}(K, V, N, s, n_1, n_2, r, c)$    ▷ First clustering after prefilling
**end if**
**Decoding:** $q, k, v \in \mathbb{R}^{1 \times d}$.
**for** $i = 1 \ldots \Gamma - 1$ **do**
    $K = [K, k]$, $V = [V, v]$, $N = [N, 1]$, $s = s + 1$.    ▷ Update the cache centroids
    $O = \text{softmax}(qK^T/\sqrt{d} + \log N) \cdot V$    ▷ Equation 3
    **if** $s \geq B + g$ **then**
        $K, V, N, s = \text{CentroidKV}(K, V, N, s, n_1, n_2, r, c)$    ▷ Clustering every $g$ decoding steps
    **end if**
**end for**
```

Table 1: Computational complexity of distance matrix. n is the sequence length and d is hidden dimension. k and i of K-Means refer to number of cluster centers and iterations. c of Chunked Soft Matching (CSM) refers to chunk size, which is relatively small to n.

Mesh	K-Means	BSM	CSM
n^2d	$inkd$	$\frac{1}{4}n^2d$	$\frac{1}{4}ncd$

5.2 Chunked Soft Matching

Based on Observation 1 in Section 4, CentroidKV begins by dividing the key states into chunks, as illustrated in Figure 1. The localized similarity of key states ensures that this approach will not cause a significant loss of accuracy. We keep the attention sink and recent tokens before partitioning, regarding their importance for model performance (Zhang et al., 2023; Xiao et al., 2023).

Inspired by the Bipartite Soft Matching (BSM) algorithm introduced by (Bolya et al., 2022) for token merging in the transformer block of Vision Transformers (ViT) (Dosovitskiy, 2020), we propose Chunked Soft Matching (CSM) for KV cache clustering in the second step of CentroidKV. BSM begins by partitioning the input tokens into two distinct sets, A and B. Next, for each token in set A, an edge is drawn to its most similar token in set B. Among these edges, only the top-ranked similar connections are retained. Tokens that remain connected through these edges are then merged into a cluster, while others are left unchanged. Finally, the two sets, A and B, are concatenated to form the output, incorporating both merged and unchanged tokens.

However, directly applying BSM for KV cache clustering poses two significant challenges. The first challenge arises from the large sequence dimension in long-context scenarios, which leads to inefficiencies in the matching process. The second challenge involves optimally partitioning the sequence into two sets, A and B, in a way that minimizes the impact on model accuracy.

CSM addresses the first challenge through a preceding chunking step, which directly improves computational efficiency. While there are alternative approaches for KV cache clustering, such as K-means, they typically require multiple iterative updates to establish stable clusters, leading to substantial computational overhead. We summarize the computational complexity of representative methods in Table 1. In particular, the “Mesh” method computes pairwise cosine similarity across all tokens, incurring significant cost. In contrast, CSM achieves the lowest complexity by performing a single-pass clustering procedure with minimal token interactions.

Building on Observation 2 in Section 4, we address the second challenge by partitioning each chunk into two sets, A and B, in an alternating manner. The core idea of CSM is to assign highly similar states to different sets, ensuring that token pairs with high similarity are placed between sets, rather than within them. Furthermore, based on the observed monotonically decreasing and convex trend, we rigorously demonstrate the theoretical optimality of this intra-chunk partitioning strategy in Section 6. After computing the similarities, CSM aggregates the edges from all chunks and prunes those with relatively low similarity scores. Finally, the clustering sets are identified as collections of tokens connected by the remaining edges.

5.3 KV Cache Compression

After cluster assignments are determined, the KV states within each cluster are merged into a centroid according to a predefined aggregation rule. As shown in Algorithm 1, clustering is performed over multiple rounds; therefore, we maintain a degree counter n_t for each cluster to track its cumulative contribution. Within each cluster, both key and value states are aggregated using degree-weighted averaging. Specifically, for a cluster $k_1, k_2, \dots, k_t$ with corresponding degrees $n_1, n_2, \dots, n_t$, the centroid of the key states is computed as:

$$\hat{k} = \frac{n_1 k_1 + n_2 k_2 + \cdots + n_t k_t}{n_1 + n_2 + \cdots + n_t} \tag{4}$$

Value states are merged analogously using the same degree-based weighting. The resulting compressed key and value centroids are then concatenated with the preserved attention sink and recent tokens to form the compressed KV cache for the subsequent decoding step.

6 Theoretical Results

In this section, we theoretically justify the optimality of our partitioning strategy which divides each chunk into two sets A and B in an alternating manner.

Intuitively, the partitioning strategy should retain the edges with the highest similarities to yield better clusters. Based on Observation 2 in Section 4, we consider a convex and monotonically decreasing score function $f : \mathbb{N} \to \mathbb{R}$ that maps the distance to an importance score. With the score function f, the optimal partitioning can be achieved by solving the following optimization problem:

$$\max_{A,B} \quad \sum_{x \in A} \sum_{y \in B} f(|x - y|). \tag{5}$$

The following theorem states that, for any score function f that is convex and monotonically decreasing, the alternating partitioning strategy we propose is always the optimal solution of problem Equation (5). Detailed proof is illustrated in Appendix A.

Theorem 6.1. *Define partition set $\mathcal{P}_{2n} = \{(A, B) \mid |A| = |B| = n, \text{ and } A \cup B = [2n]\}$. If function $f : [2n-1] \to \mathbb{R}$ satisfies $f(1) - f(2) \geq f(2) - f(3) \geq \cdots \geq f(2n-2) - f(2n-1) \geq 0$, it holds that*

$$\begin{aligned}(A_0, B_0) =& (\{1, 3, \cdots, 2n-1\}, \{2, 4, \cdots, 2n\}) \\ &\in \arg\max_{(A,B) \in \mathcal{P}_{2n}} \sum_{x \in A} \sum_{y \in B} f(|x - y|).\end{aligned}$$

Here, we use notation $[k]$ to denote the set of positive integers no larger than k, i.e., $[k] := [1, k] \cap \mathbb{Z}$.

7 Experiments

In this section, we conduct comprehensive experiments to evaluate the effectiveness and efficiency of CentroidKV, followed by the ablation study on the framework design.

Table 2: Detailed comparison of RULER benchmark datasets across various budgets on Llama-3.1-8B-Instruct.

Budget	Method	CWE	FWE	MK-NIAH-1	MK-NIAH-2	MK-NIAH-3	MQ-NIAH	MV-NIAH	S-NIAH-1	S-NIAH-2	S-NIAH-3	QA-1	QA-2	VT
100%	Full	99.31	95.80	100.00	100.00	100.00	100.00	100.00	100.00	100.00	100.00	88.24	56.67	99.77
75%	StreamingLLM	**99.71**	93.99	84.62	80.68	**75.00**	76.52	77.31	79.51	77.06	71.91	**87.25**	51.11	94.32
	SnapKV	99.02	95.20	98.08	81.82	56.82	95.45	89.58	98.36	100.00	10.11	84.31	51.11	92.73
	PyramidKV	99.51	93.69	98.08	85.23	53.41	98.23	97.92	99.18	100.00	10.11	86.27	47.78	95.91
	CentroidKV	99.12	**95.20**	**100.00**	**100.00**	60.23	**99.75**	**98.61**	**100.00**	**100.00**	**87.64**	84.31	**54.44**	**99.32**
50%	StreamingLLM	58.04	91.59	54.81	46.59	**51.14**	53.54	52.78	48.36	42.20	**53.93**	**87.25**	47.78	73.64
	SnapKV	**98.53**	92.49	91.35	47.73	22.73	78.03	73.38	95.08	93.58	2.25	73.53	43.33	80.68
	PyramidKV	88.63	90.39	85.58	57.95	18.18	76.01	77.78	96.72	97.25	1.12	73.53	43.33	81.82
	CentroidKV	97.45	**93.39**	**99.04**	**81.82**	4.55	**97.47**	**92.13**	**100.00**	**100.00**	37.08	78.43	**52.22**	**96.59**
25%	StreamingLLM	10.29	**93.39**	32.69	22.73	**21.59**	29.04	26.85	27.87	19.27	**28.09**	**89.22**	**38.89**	43.64
	SnapKV	86.08	85.59	33.65	10.23	1.14	24.75	24.07	80.33	53.21	1.12	55.88	27.78	59.32
	PyramidKV	**86.27**	85.59	33.65	10.23	1.14	23.23	24.07	80.33	53.21	1.12	55.88	26.67	59.32
	CentroidKV	85.10	87.69	**87.50**	**23.86**	0.00	**77.27**	**67.36**	**100.00**	**96.33**	3.37	36.27	30.00	**88.64**

7.1 Experimental Settings

Models and baselines. We employ two long-context models: Llama-3.1-8B-Instruct (Meta, 2024) and Mistral-7B-Instruct-v0.2 (Jiang et al., 2023), serving as the backbone LLMs. We compare CentroidKV against state-of-the-art KV cache compression methods, including StreamingLLM (Xiao et al., 2023), SnapKV (Li et al., 2024) and PyramidKV (Cai et al., 2024).

Datasets. We evaluate CentroidKV using the widely recognized benchmarks: RULER (Hsieh et al., 2024) and LongBench (Bai et al., 2023). As the variation of the Needle-in-a-Haystack test (Kamradt, 2024), RULER includes 13 long-sequence tasks designed to assess the long-context understanding capabilities of LLMs. Additionally, LongBench includes tasks covering various application scenarios: single-document QA, multi-document QA, summarization, few-shot learning, synthetic tasks, and code completion.

Implementation Details. We implement all methods in the HuggingFace Transformers codebase (Wolf, 2019). Following KVPress (Devoto et al., 2025), each input is divided into context and question segments. In our evaluation protocol, only the context is available during compression, while the question is introduced afterward for answer generation. This setup more faithfully reflects real-world deployment, where future queries are unknown at compression time, and therefore constitutes a more challenging and realistic setting. Unless otherwise specified, CentroidKV uses 16 attention sinks and retains 64 recent tokens. The compression ratio is set to 0.8 for the first clustering round. The default chunk size is 256, and all computations are performed in bfloat16 precision. Unless otherwise specified, experiments on RULER use a default context length of 4K tokens. All experiments are conducted on high-performance GPUs delivering over 100 TFLOPS of compute.

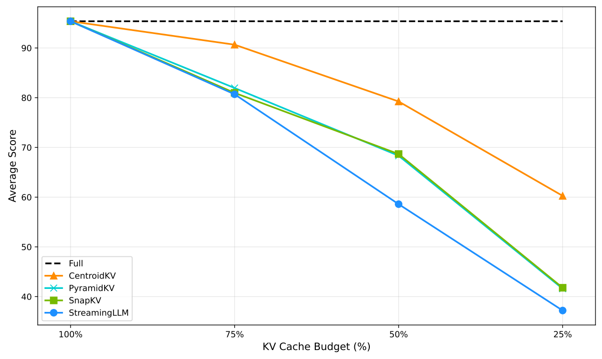

(a) Llama-3.1-8B-Instruct

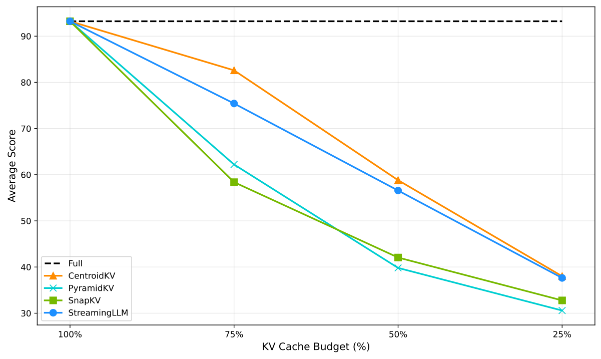

(b) Mistral-7B-Instruct-v0.2

Figure 4: Average score comparison of RULER benchmark across different cache budgets.

Table 3: Performance comparison of compression methods across various budgets for Ruler Mistral model.

Budget	Method	CWE	FWE	MK-NIAH-1	MK-NIAH-2	MK-NIAH-3	MQ-NIAH	MV-NIAH	S-NIAH-1	S-NIAH-2	S-NIAH-3	QA-1	QA-2	VT
100%	Full	95.88	92.79	99.04	100.00	93.18	98.48	87.27	100.00	99.08	98.88	86.27	62.22	98.86
75%	StreamingLLM	92.75	**91.89**	84.62	80.68	**68.18**	65.91	**73.38**	79.51	**77.06**	70.79	**86.27**	56.67	52.73
	SnapKV	95.00	90.99	38.46	76.14	67.05	32.32	25.00	87.70	67.89	6.74	85.29	58.89	27.50
	PyramidKV	**95.98**	90.99	47.12	76.14	57.95	38.13	30.79	93.44	69.72	6.74	84.31	**62.22**	55.23
	CentroidKV	94.02	90.69	**87.50**	**97.73**	54.55	**79.80**	65.97	**100.00**	71.56	**96.63**	83.33	53.33	**98.64**
50%	StreamingLLM	90.98	**89.79**	54.81	46.59	**40.91**	33.08	**52.08**	46.72	**42.20**	52.81	**87.25**	47.78	50.45
	SnapKV	**94.31**	88.89	23.08	44.32	17.05	15.40	14.58	78.69	22.02	2.25	76.47	51.11	18.64
	PyramidKV	79.80	86.79	20.19	39.77	9.09	13.64	13.89	86.89	15.60	1.12	70.59	**51.11**	29.09
	CentroidKV	89.31	88.29	**57.69**	**56.82**	2.27	**34.09**	29.86	**100.00**	36.70	**53.93**	71.57	46.67	**97.27**
25%	StreamingLLM	60.20	**90.99**	**32.69**	**21.59**	**18.18**	**16.67**	**26.16**	27.87	**19.27**	**28.09**	**88.24**	**40.00**	19.32
	SnapKV	**87.35**	84.08	14.42	14.77	0.00	13.89	14.35	69.67	11.01	1.12	60.78	38.89	15.68
	PyramidKV	58.92	84.38	14.42	14.77	0.00	13.38	14.35	69.67	11.01	1.12	60.78	38.89	15.91
	CentroidKV	76.57	74.77	17.31	11.36	0.00	5.30	9.49	**100.00**	15.60	3.37	51.96	34.44	**94.09**

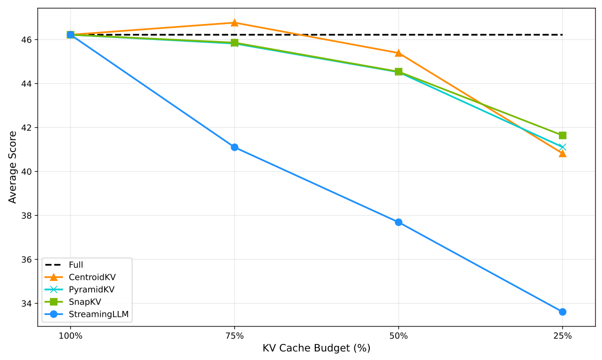

(a) Llama-3.1-8B-Instruct

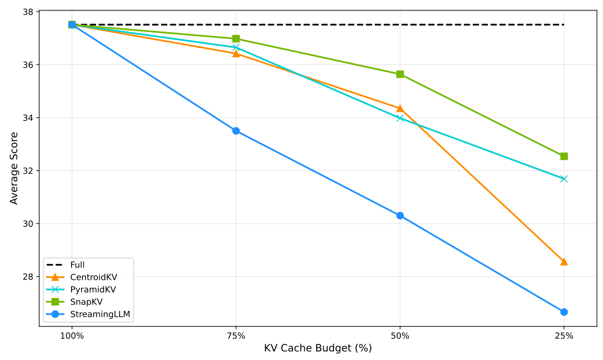

(b) Mistral-7B-Instruct-v0.2

Figure 5: Average score comparison of LongBench tasks across different cache budgets.

7.2 Accuracy Evaluation

We evaluate model accuracy under different KV cache compression methods on RULER and LongBench. We report results under cache budgets of 75%, 50%, and 25% relative to the full KV cache.

RULER. Figure 4 summarizes the average scores across 13 RULER datasets under different KV cache budgets. CentroidKV consistently achieves the strongest overall performance across both Llama-3.1-8B-Instruct and Mistral-7B-Instruct-v0.2. Notably, performance gaps widen as the cache budget decreases, highlighting the robustness of CentroidKV under aggressive compression. At the most challenging 25% budget, CentroidKV preserves substantially higher accuracy compared to alternative compression strategies, whereas competing methods exhibit significant degradation. Detailed per-task results in Table 2 and Table 3 further confirm this trend. CentroidKV achieves the best or near-best results on the majority of datasets across all budgets, particularly excelling on Single NIAH (S-NIAH) and Multi-keys NIAH (MK-NIAH). In scenarios where other baselines achieve higher score, CentroidKV maintains more stable performance across tasks, resulting in superior overall averages and improved worst-case behavior.

LongBench. Figure 5 reports average performance across 16 LongBench tasks. On Llama-3.1-8B-Instruct, CentroidKV consistently provides the most favorable accuracy–compression trade-off across all budgets, maintaining strong performance even under substantial cache reduction. The stability of CentroidKV across diverse tasks underscores its generalizability. On Mistral-7B-Instruct-v0.2, while PyramidKV and SnapKV obtain slightly higher average scores under the extreme 25% budget, a closer inspection reveals that the gap is driven by a small subset of tasks. As shown in Table 5, performance differences primarily arise from few-shot Learning tasks TREC, TriviaQA and synthetic task PassageRetrieval. Outside these outliers, CentroidKV achieves competitive or leading performance across many datasets and maintains strong robustness across heterogeneous tasks. Moreover, the corresponding Llama results in Table 4 show that such

Table 4: Detailed results of LongBench datasets with 25% KV cache budget on Llama-3.1-8B-Instruct.

Dataset	StreamingLLM	SnapKV	PyramidKV	CentroidKV	Full
2WikiMQA	27.92	**42.44**	39.83	33.18	51.33
GovReport	28.79	**29.24**	28.23	27.24	35.19
HotpotQA	41.95	**55.18**	55.13	52.08	59.80
LCC	50.84	**53.83**	53.61	51.21	53.31
MultiNews	**23.91**	23.35	23.41	23.10	26.99
MultiFieldQA-en	25.62	35.01	34.79	**39.81**	56.31
Musique	20.07	**28.18**	25.19	25.58	33.51
NarrativeQA	23.25	**28.43**	26.92	27.03	30.99
Passage Count	7.00	9.10	9.55	**10.00**	10.70
PassageRetrieval-en	33.50	90.00	**93.50**	92.00	100.00
Qasper	24.38	31.36	30.08	**33.27**	47.39
QMSum	20.69	22.41	22.20	**23.42**	25.34
RepoBench-P	**50.50**	47.72	47.28	49.30	47.23
SAMSum	35.70	41.43	**42.26**	41.74	40.77
TREC	31.50	**37.00**	34.00	33.00	29.00
TriviaQA	**92.12**	91.54	91.73	91.14	91.71

Table 5: Detailed results of LongBench datasets with 25% KV cache budget on Mistral-7B-Instruct-v0.2.

Dataset	StreamingLLM	SnapKV	PyramidKV	CentroidKV	Full
2WikiMQA	**15.83**	13.75	13.59	15.62	20.97
GovReport	**28.38**	27.27	26.20	26.87	32.34
HotpotQA	21.59	23.96	22.98	**25.98**	35.34
LCC	48.37	**51.25**	50.79	47.34	51.35
MultiNews	22.87	23.16	23.23	**23.60**	26.55
MultiFieldQA-en	22.46	31.65	31.27	**32.20**	45.94
Musique	10.42	**11.32**	10.03	9.68	17.30
NarrativeQA	21.36	18.62	17.30	**21.42**	23.86
Passage Count	3.10	**3.91**	3.39	2.94	2.48
PassageRetrieval-en	18.48	**68.81**	66.77	35.32	73.76
Qasper	13.32	14.36	13.57	**15.45**	29.20
QMSum	20.58	21.59	21.41	**22.94**	24.37
RepoBench-P	47.55	**51.08**	50.74	50.09	51.16
SAMSum	36.12	38.68	**39.10**	36.63	39.61
TREC	**47.50**	41.75	39.25	23.50	51.25
TriviaQA	48.69	**79.43**	77.46	67.37	74.68

gaps are substantially smaller or disappear entirely, reinforcing the consistency of CentroidKV across different model architectures.

Summary. Across both RULER and LongBench benchmarks, CentroidKV delivers the most reliable performance under constrained KV cache budgets. It consistently achieves higher average accuracy, stronger robustness under extreme compression, and more balanced performance across diverse task scenarios. These results demonstrate that CentroidKV provides an effective solution for preserving model capability under long-context memory constraints.

7.3 Efficiency Evaluation

We evaluate inference efficiency by decoding latency and GPU memory consumption. We report two standard latency metrics: Time To First Token (TTFT), which reflects the pre-filling overhead, and Time

Table 6: Decoding latency and GPU memory usage comparison across varying context lengths on Llama-3.1-8B-Instruct. TTFT(s) and TPOT(s) are based on HuggingFace Transformers.

Context Length	Method	TTFT	TPOT	Speedup ↑	Memory (GB)
16k	Full	1.784	0.043	/	19.38
	CentroidKV	1.814	**0.035**	**1.23**×	15.86
32k	Full	4.212	0.071	/	23.53
	CentroidKV	4.306	**0.036**	**1.97**×	16.69
64k	Full	11.421	0.137	/	31.83
	CentroidKV	11.500	**0.043**	**3.19**×	18.36

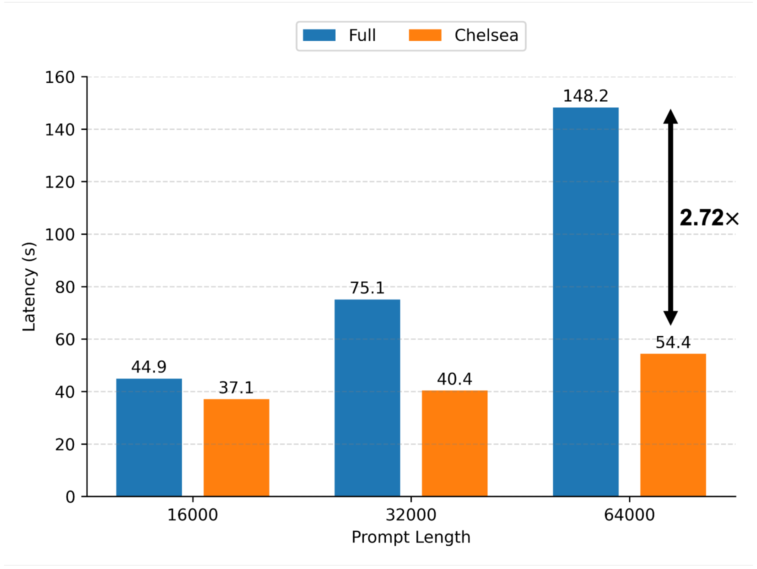

Figure 6: End-to-end latency with a decoding length of 1000 tokens on Llama-3.1-8B-Instruct.

Per Output Token (TPOT), which directly measures decoding efficiency. All measurements are conducted on Llama-3.1-8B-Instruct using the HuggingFace Transformers framework.

Latency. Table 6 summarizes latency and memory statistics across increasing context lengths. CentroidKV introduces negligible overhead during the pre-filling stage, with TTFT remaining comparable to full attention even at long contexts. In contrast, it substantially reduces TPOT, yielding consistent and increasing decoding speedups as context length grows. At 64K context length, CentroidKV achieves a 3.19× decoding speedup over full attention, demonstrating its effectiveness in mitigating the quadratic cost of long-context decoding. Figure 6 reports end-to-end latency with a fixed decoding length of 1000 tokens. At 64K tokens, CentroidKV reduces end-to-end latency by up to 2.72×, confirming that improvements in TPOT translate directly into real-world inference speedups.

Memory. In addition to latency improvements, CentroidKV significantly reduces GPU memory usage. Compared to full attention, memory consumption is reduced from 31.83 GB to 18.36 GB at 64K context length, enabling long-context inference on more resource-constrained hardware.

Overall, CentroidKV delivers substantial decoding acceleration and memory savings while preserving pre-filling efficiency. Its speedup scales favorably with context length, making it particularly well-suited for long-context inference scenarios where decoding dominates runtime.

Table 7: TTFT (s) and TPOT (s) on Llama-3.1-8B-Instruct based on HuggingFace Transformers. The clustering overhead is largely reduced by chunking.

	Context Length	**16k**		**32k**		**64k**		
	Full	1.784	0.043	4.212	0.071	**11.421**	0.137	Overhead (s) ↓
Chunking	×	1.842	0.035	4.526	0.036	**13.156**	0.044	+1.735
	✓	1.814	0.035	4.306	0.036	**11.500**	0.043	+0.079

Table 8: Performance of CentroidKV with different chunk size. Chunk size has a relatively small effect on accuracy within a certain range.

Chunk Size	16	64	256	w/o chunk
Avg. Score	41.83	42.68	42.54	42.81

7.4 Ablation Study

We conduct ablation experiments to analyze the role of the key chunking mechanism in CentroidKV. Chunking is applied prior to soft matching to reduce clustering complexity and improve practical efficiency. We evaluate its impact on both inference latency and model accuracy.

Beyond the theoretical complexity analysis presented in Table 1, we empirically measure the runtime overhead introduced by clustering. Table 7 compares latency with and without chunking across increasing context lengths. Without chunking, clustering introduces substantial overhead, particularly at long contexts (e.g., +1.735 s at 64K), which partially offsets decoding gains. In contrast, chunking significantly reduces the additional cost to a negligible level (+0.079 s at 64K), while maintaining comparable TTFT and TPOT improvements. These results demonstrate that chunking is critical for achieving scalable acceleration in long-context scenarios.

We further evaluate the sensitivity of CentroidKV to different chunk sizes using subsets of LongBench. As shown in Table 8, performance remains stable across a wide range of chunk sizes, with only minor fluctuations in average scores. The results indicate that chunking does not significantly degrade contextual representation within practical parameter ranges.

8 Conclusion and Limitations

This paper presents CentroidKV, a simple yet effective framework for online KV cache clustering that improves the efficiency of long-context LLM inference. CentroidKV reduces KV cache memory usage by up to 75% without compromising accuracy on most tasks, while accelerating the decoding stage by up to 3.19× and reducing end-to-end latency by up to 2.72×. However, our work focuses on compressing the KV cache on the GPU and does not investigate memory offloading strategies. A promising direction for future research is to perform clustering on the CPU and transfer the resulting centroids to the GPU. Additionally, CentroidKV currently employs a manually specified, static compression ratio and restricts cache reduction to at most half at each clustering step. This could be addressed by designing a dynamic compression strategy in future work.

References

Josh Achiam, Steven Adler, Sandhini Agarwal, Lama Ahmad, Ilge Akkaya, Florencia Leoni Aleman, Diogo Almeida, Janko Altenschmidt, Sam Altman, Shyamal Anadkat, et al. Gpt-4 technical report. *arXiv preprint arXiv:2303.08774*, 2023.

Yushi Bai, Xin Lv, Jiajie Zhang, Hongchang Lyu, Jiankai Tang, Zhidian Huang, Zhengxiao Du, Xiao Liu, Aohan Zeng, Lei Hou, et al. Longbench: A bilingual, multitask benchmark for long context understanding. *arXiv preprint arXiv:2308.14508*, 2023.

Daniel Bolya and Judy Hoffman. Token merging for fast stable diffusion. In *Proceedings of the IEEE/CVF conference on computer vision and pattern recognition*, pp. 4599–4603, 2023.

Daniel Bolya, Cheng-Yang Fu, Xiaoliang Dai, Peizhao Zhang, Christoph Feichtenhofer, and Judy Hoffman. Token merging: Your vit but faster. *arXiv preprint arXiv:2210.09461*, 2022.

Zefan Cai, Yichi Zhang, Bofei Gao, Yuliang Liu, Tianyu Liu, Keming Lu, Wayne Xiong, Yue Dong, Baobao Chang, Junjie Hu, et al. Pyramidkv: Dynamic kv cache compression based on pyramidal information funneling. *arXiv preprint arXiv:2406.02069*, 2024.

Tri Dao, Dan Fu, Stefano Ermon, Atri Rudra, and Christopher Ré. Flashattention: Fast and memory-efficient exact attention with io-awareness. *Advances in Neural Information Processing Systems*, 35:16344–16359, 2022.

Alessio Devoto, Maximilian Jeblick, and Simon Jégou. Expected attention: Kv cache compression by estimating attention from future queries distribution. *arXiv preprint arXiv:2510.00636*, 2025. URL `https://arxiv.org/abs/2510.00636`.

Alexey Dosovitskiy. An image is worth 16x16 words: Transformers for image recognition at scale. *arXiv preprint arXiv:2010.11929*, 2020.

Yuan Feng, Junlin Lv, Yukun Cao, Xike Xie, and S Kevin Zhou. Ada-kv: Optimizing kv cache eviction by adaptive budget allocation for efficient llm inference. *arXiv preprint arXiv:2407.11550*, 2024.

Suyu Ge, Yunan Zhang, Liyuan Liu, Minjia Zhang, Jiawei Han, and Jianfeng Gao. Model tells you what to discard: Adaptive kv cache compression for llms. *arXiv preprint arXiv:2310.01801*, 2023.

Coleman Hooper, Sehoon Kim, Hiva Mohammadzadeh, Michael W Mahoney, Yakun Sophia Shao, Kurt Keutzer, and Amir Gholami. Kvquant: Towards 10 million context length llm inference with kv cache quantization. *arXiv preprint arXiv:2401.18079*, 2024.

Cheng-Ping Hsieh, Simeng Sun, Samuel Kriman, Shantanu Acharya, Dima Rekesh, Fei Jia, Yang Zhang, and Boris Ginsburg. Ruler: What's the real context size of your long-context language models? *arXiv preprint arXiv:2404.06654*, 2024.

Albert Q. Jiang, Alexandre Sablayrolles, Arthur Mensch, Chris Bamford, Devendra Singh Chaplot, Diego de las Casas, Florian Bressand, Gianna Lengyel, Guillaume Lample, Lucile Saulnier, Lélio Renard Lavaud, Marie-Anne Lachaux, Pierre Stock, Teven Le Scao, Thibaut Lavril, Thomas Wang, Timothée Lacroix, and William El Sayed. Mistral 7b, 2023. URL `https://arxiv.org/abs/2310.06825`.

Greg Kamradt. Needle in a haystack: Evaluating long-context retrieval in language models. Online, 2024. URL `https://github.com/gkamradt/LLMTest_NeedleInAHaystack`. A benchmark for testing LLMs' ability to retrieve specific information from long-context inputs.

Minchul Kim, Shangqian Gao, Yen-Chang Hsu, Yilin Shen, and Hongxia Jin. Token fusion: Bridging the gap between token pruning and token merging. In *Proceedings of the IEEE/CVF Winter Conference on Applications of Computer Vision*, pp. 1383–1392, 2024.

Yuhong Li, Yingbing Huang, Bowen Yang, Bharat Venkitesh, Acyr Locatelli, Hanchen Ye, Tianle Cai, Patrick Lewis, and Deming Chen. Snapkv: Llm knows what you are looking for before generation. *arXiv preprint arXiv:2404.14469*, 2024.

Guangda Liu, Chengwei Li, Jieru Zhao, Chenqi Zhang, and Minyi Guo. Clusterkv: Manipulating llm kv cache in semantic space for recallable compression. *arXiv preprint arXiv:2412.03213*, 2024a.

Zichang Liu, Aditya Desai, Fangshuo Liao, Weitao Wang, Victor Xie, Zhaozhuo Xu, Anastasios Kyrillidis, and Anshumali Shrivastava. Scissorhands: Exploiting the persistence of importance hypothesis for llm kv cache compression at test time. *Advances in Neural Information Processing Systems*, 36, 2024b.

Zirui Liu, Jiayi Yuan, Hongye Jin, Shaochen Zhong, Zhaozhuo Xu, Vladimir Braverman, Beidi Chen, and Xia Hu. Kivi: A tuning-free asymmetric 2bit quantization for kv cache. *arXiv preprint arXiv:2402.02750*, 2024c.

Stephen Merity, Caiming Xiong, James Bradbury, and Richard Socher. Pointer sentinel mixture models. *arXiv preprint arXiv:1609.07843*, 2016.

AI Meta. Introducing meta llama 3: The most capable openly available llm to date. *Meta AI*, 2024.

Robin Rombach, Andreas Blattmann, Dominik Lorenz, Patrick Esser, and Björn Ommer. High-resolution image synthesis with latent diffusion models. In *Proceedings of the IEEE/CVF conference on computer vision and pattern recognition*, pp. 10684–10695, 2022.

Zhenmei Shi, Yifei Ming, Xuan-Phi Nguyen, Yingyu Liang, and Shafiq Joty. Discovering the gems in early layers: Accelerating long-context llms with 1000x input token reduction. *arXiv preprint arXiv:2409.17422*, 2024.

Hanlin Tang, Yang Lin, Jing Lin, Qingsen Han, Shikuan Hong, Yiwu Yao, and Gongyi Wang. Razorattention: Efficient kv cache compression through retrieval heads. *arXiv preprint arXiv:2407.15891*, 2024.

Gemini Team, Petko Georgiev, Ving Ian Lei, Ryan Burnell, Libin Bai, Anmol Gulati, Garrett Tanzer, Damien Vincent, Zhufeng Pan, Shibo Wang, et al. Gemini 1.5: Unlocking multimodal understanding across millions of tokens of context. *arXiv preprint arXiv:2403.05530*, 2024.

Rajarshi Thoppilan, Fang Xu, Chunyang Chen, Yifan Luan, Shuang Zhang, and Ilya Sutskever. Chatgpt: Optimizing language models for dialogue. *OpenAI Blog*, 2022. URL `https://openai.com/research/chatgpt-optimizing-language-models-for-dialogue`.

Together. Llama-2-7b-32k-instruct — and fine-tuning for llama-2 models with together api, June 2023. URL `https://www.together.ai/blog/llama-2-7b-32k-instruct`.

Hugo Touvron, Thibaut Lavril, Gautier Izacard, Xavier Martinet, Marie-Anne Lachaux, Timothée Lacroix, Baptiste Rozière, Naman Goyal, Eric Hambro, Faisal Azhar, et al. Llama: Open and efficient foundation language models. *arXiv preprint arXiv:2302.13971*, 2023.

Hoai-Chau Tran, Duy MH Nguyen, Duy M Nguyen, Trung-Tin Nguyen, Ngan Le, Pengtao Xie, Daniel Sonntag, James Y Zou, Binh T Nguyen, and Mathias Niepert. Accelerating transformers with spectrum-preserving token merging. *arXiv preprint arXiv:2405.16148*, 2024.

Zhongwei Wan, Xinjian Wu, Yu Zhang, Yi Xin, Chaofan Tao, Zhihong Zhu, Xin Wang, Siqi Luo, Jing Xiong, and Mi Zhang. D2o: Dynamic discriminative operations for efficient generative inference of large language models. *arXiv preprint arXiv:2406.13035*, 2024.

Zheng Wang, Boxiao Jin, Zhongzhi Yu, and Minjia Zhang. Model tells you where to merge: Adaptive kv cache merging for llms on long-context tasks. *arXiv preprint arXiv:2407.08454*, 2024.

T Wolf. Huggingface's transformers: State-of-the-art natural language processing. *arXiv preprint arXiv:1910.03771*, 2019.

Guangxuan Xiao, Yuandong Tian, Beidi Chen, Song Han, and Mike Lewis. Efficient streaming language models with attention sinks. *arXiv preprint arXiv:2309.17453*, 2023.

Guangxuan Xiao, Jiaming Tang, Jingwei Zuo, Junxian Guo, Shang Yang, Haotian Tang, Yao Fu, and Song Han. Duoattention: Efficient long-context llm inference with retrieval and streaming heads. *arXiv preprint arXiv:2410.10819*, 2024.

Yuhui Xu, Zhanming Jie, Hanze Dong, Lei Wang, Xudong Lu, Aojun Zhou, Amrita Saha, Caiming Xiong, and Doyen Sahoo. Think: Thinner key cache by query-driven pruning. *arXiv preprint arXiv:2407.21018*, 2024.

Dongjie Yang, XiaoDong Han, Yan Gao, Yao Hu, Shilin Zhang, and Hai Zhao. Pyramidinfer: Pyramid kv cache compression for high-throughput llm inference. *arXiv preprint arXiv:2405.12532*, 2024.

Yuxin Zhang, Yuxuan Du, Gen Luo, Yunshan Zhong, Zhenyu Zhang, Shiwei Liu, and Rongrong Ji. Cam: Cache merging for memory-efficient llms inference. In *Forty-first International Conference on Machine Learning*.

Zhenyu Zhang, Ying Sheng, Tianyi Zhou, Tianlong Chen, Lianmin Zheng, Ruisi Cai, Zhao Song, Yuandong Tian, Christopher Ré, Clark Barrett, et al. H2o: Heavy-hitter oracle for efficient generative inference of large language models. *Advances in Neural Information Processing Systems*, 36:34661–34710, 2023.

A Proof of Theorem 6.1

Proof. When $n = 1$, the result is trivial. In the following, we assume $n \geq 2$. Consider the following mapping:

$$\begin{aligned}\phi_{2n} : \mathbb{Z} \to & [2n] \\ x \mapsto & \begin{cases} 1, & x < 1; \\ x, & x \in [2n]; \\ 2n, & x > 2n; \end{cases}\end{aligned}$$

For any $l \in [2n-1]$, define $\mathcal{S}_{2n,l} := \{(\phi_{2n}(x), \phi_{2n}(x+l)) \mid x \in \mathbb{Z} \cap [-l+2, 2n-1]\}$. For $\forall (A, B) \in \mathcal{P}_{2n}$, define

$$\mathcal{E}_{A,B} := \{(\min\{a,b\}, \max\{a,b\}) \mid a \in A \text{ and } b \in B\}, \tag{6}$$

$$\mathcal{D}_{A,B,l} := \{(a,b) \in \mathcal{E}_{A,B} \mid b - a = l\}, \tag{7}$$

$$\mathcal{T}_{A,B,l} := \{(a,b;c,d) \in [2n]^4 \mid (a,b) \in \mathcal{S}_{2n,l},\ (c,d) \in \mathcal{E}_{A,B},\ \text{and } [c,d] \subseteq [a,b]\}, \tag{8}$$

Now we calculate the number of elements in $\mathcal{T}_{A,B,l}$, *i.e.*, $|\mathcal{T}_{A,B,l}|$. Define $\mathcal{K}_{A,B,a,b} := \{(c,d) \in \mathcal{E}_{A,B} \mid [c,d] \subseteq [a,b]\}$, it holds that

$$|\mathcal{T}_{A,B,l}| = \sum_{(a,b) \in \mathcal{S}_{2n,l}} |\mathcal{K}_{A,B,a,b}|. \tag{9}$$

Note that

$$|\mathcal{K}_{A,B,a,b}| = |[a,b] \cap A| \cdot |[a,b] \cap B| \leq \left\lfloor \frac{b-a+1}{2} \right\rfloor \cdot \left\lceil \frac{b-a+1}{2} \right\rceil, \tag{10}$$

applying equation 10 to equation 9 yields

$$\begin{aligned} |\mathcal{T}_{A,B,l}| \leq & \sum_{(a,b) \in \mathcal{S}_{2n,l}} \left\lfloor \frac{b-a+1}{2} \right\rfloor \cdot \left\lceil \frac{b-a+1}{2} \right\rceil \\ = & \sum_{i=2}^{l} \left\lfloor \frac{i-1+1}{2} \right\rfloor \cdot \left\lceil \frac{i-1+1}{2} \right\rceil + \sum_{i=1}^{2n-l} \left\lfloor \frac{(i+l)-i+1}{2} \right\rfloor \cdot \left\lceil \frac{(i+l)-i+1}{2} \right\rceil + \\ & + \sum_{i=2n-l+1}^{2n-1} \left\lfloor \frac{2n-i+1}{2} \right\rfloor \cdot \left\lceil \frac{2n-i+1}{2} \right\rceil \\ = & \begin{cases} -\frac{1}{12}l^3 + \frac{2n-1}{4}l^2 + \frac{6n-1}{6}l, & 2 \mid l; \\ -\frac{1}{12}l^3 + \frac{2n-1}{4}l^2 + \frac{12n-5}{12}l + \frac{2n-1}{4}, & 2 \nmid l. \end{cases} \triangleq c_{2n,l}. \end{aligned} \tag{11}$$

On the other hand, define $\mathcal{K}'_{2n,l,c,d} := \{(a,b) \in \mathcal{S}_{2n,l} \mid [c,d] \subseteq [a,b]\}$, we have

$$|\mathcal{K}'_{2n,l,c,d}| = \max(l+1-d+c, 0),$$

thus

$$\begin{aligned} |\mathcal{T}_{A,B,l}| &= \sum_{(c,d)\in\mathcal{E}_{A,B}} |\mathcal{K}'_{2n,l,c,d}| \\ &= \sum_{(c,d)\in\mathcal{E}_{A,B}} \max(l+1-d+c, 0) \\ &= \sum_{i=1}^{l} (l+1-i)|\mathcal{D}_{A,B,i}|. \end{aligned} \tag{12}$$

Combining equation 11equation 12 yields

$$\sum_{i=1}^{l} (l+1-i)|\mathcal{D}_{A,B,i}| \le c_{2n,l}. \tag{13}$$

Define $a_i = f(i) - f(i+1)$ for $i \in [2n-2]$, $b_i = a_i - a_{i+1}$ for $i \in [2n-3]$, and let $b_{2n-2} = a_{2n-2}$, it holds that $b_1, b_2, \cdots, b_{2n-2} \ge 0$. Note that

$$\begin{aligned} f(i) =& f(2n-1) + \sum_{j=i}^{2n-2} a_j, \\ =& f(2n-1) + \sum_{j=i}^{2n-2} \sum_{k=j}^{2n-2} b_k, \\ =& f(2n-1) + \sum_{j=i}^{2n-2} (j-i+1) b_j, \quad \forall i \in [2n-2], \end{aligned}$$

we have

$$\begin{aligned} \sum_{x\in A}\sum_{y\in B} f(|x-y|) &= \sum_{i=1}^{2n-1} |\mathcal{D}_{A,B,i}| f(i) \\ &= \sum_{i=1}^{2n-1} |\mathcal{D}_{A,B,i}| \left(f(2n-1) + \sum_{j=i}^{2n-2} (j-i+1) b_j \right) \\ &= |\mathcal{E}_{A,B}| f(2n-1) + \sum_{j=1}^{2n-2} \sum_{i=1}^{j} (j+1-i) |\mathcal{D}_{A,B,i}| b_j \\ &\le n^2 f(2n-1) + \sum_{j=1}^{2n-2} c_{2n,j} b_j, \end{aligned} \tag{14}$$

where the last inequality uses $|\mathcal{E}_{A,B}| = n^2$ and equation 13. If $A_0 = \{1, 3, \cdots, 2n-1\}$ and $B_0 = \{2, 4, \cdots, 2n\}$, we have

$$\begin{aligned} \sum_{x\in A_0}\sum_{y\in B_0} f(|x-y|) &= \sum_{i=1}^{2n-1} |\mathcal{D}_{A_0,B_0,i}| f(i) = \sum_{i=1}^{n} |\mathcal{D}_{A_0,B_0,2i-1}| f(2i-1) \\ &= \sum_{i=1}^{n} (2n-2i+1) \left(f(2n-1) + \sum_{j=2i-1}^{2n-2} (j-2i+2) b_j \right) \\ &= n^2 f(2n-1) + \sum_{j=1}^{2n-2} \sum_{i=1}^{\lfloor \frac{j+1}{2} \rfloor} (2n-2i+1)(j-2i+2) b_j. \end{aligned} \tag{15}$$

Note that

$$\sum_{i=1}^{\lfloor \frac{j+1}{2} \rfloor} (2n-2i+1)(j-2i+2) = \begin{cases} -\frac{1}{12}l^3 + \frac{2n-1}{4}l^2 + \frac{6n-1}{6}l, & 2 \mid l; \\ -\frac{1}{12}l^3 + \frac{2n-1}{4}l^2 + \frac{12n-5}{12}l + \frac{2n-1}{4}, & 2 \nmid l. \end{cases} = c_{2n,j}, \tag{16}$$

combining equation 15equation 16 yields

$$\sum_{x \in A_0} \sum_{y \in B_0} f(|x-y|) = n^2 f(2n-1) + \sum_{j=1}^{2n-2} c_{2n,j} b_j. \tag{17}$$

Combining equation 14equation 17, we obtain

$$(A_0, B_0) \in \underset{(A,B) \in \mathcal{P}_{2n}}{\arg\max} \sum_{x \in A} \sum_{y \in B} f(|x-y|),$$

which concludes the proof. □